AAC Journals.ASM.org

Praziquantel in a Clay Nanoformulation Shows More Bioavailability and Higher Efficacy against Murine *Schistosoma mansoni* Infection

Gina S. El-Feky,[a] Wael S. Mohamed,[b] Hanaa E. Nasr,[b] Naglaa M. El-Lakkany,[c] Sayed H. Seif el-Din,[c] Sanaa S. Botros[c]

Department of Pharmaceutics, Faculty of Pharmacy, October University for Modern Sciences and Arts and Department of Pharmaceutical Technology, National Research Center, Cairo, Egypt[a]; Department of Polymers and Pigments, National Research Center, Cairo, Egypt[b]; Department of Pharmacology, Theodor Bilharz Research Institute, Giza, Egypt[c]

Consideration of existing compounds always simplifies and shortens the long and difficult process of discovering new drugs specifically for diseases of developing countries, an approach that may add to the significant potential cost savings. This study focused on improving the biological characteristics of the already-existing antischistosomal praziquantel (PZQ) by incorporating it into montmorillonite (MMT) clay as a delivery carrier to overcome its known bioavailability drawbacks. The oral bioavailability of a PZQ-MMT clay nanoformulation and its *in vivo* efficacy against *Schistosoma mansoni* were investigated. The PZQ-MMT clay nanoformulation provided a preparation with a controlled release rate, a decrease in crystallinity, and an appreciable reduction in particle size. Uninfected and infected mice treated with PZQ-MMT clay showed 3.61- and 1.96-fold and 2.16- and 1.94-fold increases, respectively, in area under the concentration-time curve from 0 to 8 h (AUC_{0-8}) and maximum concentration of drug in serum (C_{max}), with a decrease in elimination rate constant (k_{el}) by 2.84- and 1.35-fold and increases in the absorption rate constant (k_a) and half-life ($t_{1/2e}$) by 2.11- and 1.51-fold and 2.86- and 1.34-fold, respectively, versus the corresponding conventional PZQ-treated groups. This improved bioavailability has been expressed in higher efficacy of the drug, where the dose necessary to kill 50% of the worms was reduced by >3-fold (PZQ 50% effective dose [ED_{50}] was 20.25 mg/kg of body weight for PZQ-MMT clay compared to 74.07 mg/kg for conventional PZQ), with significant reduction in total tissue egg load and increase in total immature, mature, and dead eggs in most of the drug-treated groups. This formulation showed better bioavailability, enhanced antischistosomal efficacy, and a safer profile despite the longer period of residence in the systemic circulation. Although the conventional drug's toxicity was not examined, animal mortality rates were not different between groups receiving the test PZQ-clay nanoformulation and conventional PZQ.

Schistosomiasis is a parasitic disease caused by blood flukes of the genus *Schistosoma* and is a serious public health problem in almost 70 countries of the tropics and subtropics without potable water and with poor sanitary conditions. It is estimated that at least 230 million people need treatment against schistosomiasis per year (1). Since an effective vaccine against schistosomiasis is lacking, the emphasis today is placed on the drug praziquantel (PZQ) (2). The low cost has made presumptive treatment on the basis of early clinical symptoms, or even universal treatment, cost-effective in many situations (3).

Although PZQ has proved to be especially useful in the treatment of schistosomiasis, it sometimes fails to give complete cures in treated populations. The failure of mass treatment to control schistosomiasis has been attributed to the fact that therapy is not sufficiently long-lasting (4). This effect can occur because of the low bioavailability of praziquantel due to its poor hydrosolubility (5). PZQ is a class II compound (high permeability, low solubility) and thus presents poor solubility in water and, consequently, low absorption through the gastrointestinal tract (GIT) (6). PZQ poor solubility restricts its delivery, especially via the oral route. Another factor that influences the effectiveness of the treatment is the pronounced rapid drug metabolism, with less effectiveness against immature worms of *Schistosoma mansoni*, which, being in systemic circulation, are less exposed to praziquantel (5), resulting in failures of mass treatment in the areas of high endemicity. Moreover, large doses are required in order to achieve adequate concentrations at larval tissue due to the high liposolubility of PZQ and its significant first-pass metabolism after oral administration, which converts PZQ to a less potent compound (7, 8).

In this respect, the argument continues that immature/larval parasites exposed to insufficient drug concentrations eventually mature and thus may be responsible for the apparently poor cure rates. Low drug concentration or, in other words, sublethal PZQ concentration is a hypothesized cause of schistosomal resistance to drug treatment (9). Another considerable concern is that complete dependence on PZQ as the sole drug for treating schistosomiasis may favor the prospects of emerging resistance to the drug (10).

Drugs developed for diseases of the poor, accounting for >1/10 of the global disease burden, comprised only 1% of the drugs developed from 1975 to 2004 (11). Nanosized novel drug delivery systems may present potential options to improve the performance of many existing drugs. Various biocompatible and biodegradable synthetic and natural polymers have been widely studied as drug delivery carriers (12) Due to its bioinert nature,

Received 14 December 2014 **Returned for modification** 7 February 2015
Accepted 29 March 2015

Accepted manuscript posted online 6 April 2015

Citation El-Feky GS, Mohamed WS, Nasr HE, El-Lakkany NM, Seif el-Din SH, Botros SS. 2015. Praziquantel in a clay nanoformulation shows more bioavailability and higher efficacy against murine *Schistosoma mansoni* infection. Antimicrob Agents Chemother 59:3501–3508. doi:10.1128/AAC.04875-14.

Address correspondence to Gina S. El-Feky, gelfeky@hotmail.com.

doi:10.1128/AAC.04875-14

fine grain, and large interlayer-planar spacing, montmorillonite (MMT) clay has been considered a potential candidate for a drug delivery carrier due to its properties in controlling drug release and improving drug solubility (13). The main objective of the present investigation is to overcome the drawbacks associated with the only current antischistosomal drug, PZQ, to reach a more effective drug therapy with minimum side effects. This will be done by incorporating the drug into MMT to enhance its oral bioavailability, thus increasing its period of residence in the systemic circulation and extending its duration of action and in turn its potency toward especially younger parasites usually exposed to lower concentrations of unchanged PZQ.

MATERIALS AND METHODS

Intercalation. In order to achieve maximum intercalation of praziquantel (kind gift from Bayer AG, Leverkusen, Germany) into the interlayer gallery of MMT (K10 montmorillonite with a specific surface area of 274 m^2/g and a cation exchange capacity of 1.2 meq/g, purchased from Sigma-Aldrich, St. Louis, MO, USA), intercalation conditions such as intercalation time (0.25, 0.5, 1, 2, 4, 8, and 12 h) and pH (2 to 9) were investigated at 60°C.

(i) Effect of time. To optimize the time required for maximum intercalation of praziquantel into the interlayer of MMT clay, 100 ml aqueous solution containing 250 mg of the drug was mixed with 250 mg clay powder for 0.25, 0.5, 1, 2, 4, 8, and 12 h at a constant pH of 2 and a constant temperature of 60°C and under continuous stirring, The reaction mixtures were then filtered, and the concentration of drug in the filtrate was determined in triplicate using UV spectroscopy at a maximum λ (λ_{max}) of 263.8 nm versus blank.

(ii) Effect of pH. To determine the optimum pH for the intercalation process of praziquantel into MMT clay, 100 ml aqueous solution containing 250 mg of drug was mixed with 250 mg clay powder at different pH values (2 to 9) at a constant temperature of 60°C for 2 h and under continuous stirring. The reaction mixtures were then filtered, and the concentration of drug in the filtrate was determined in triplicate using UV spectroscopy at a λ_{max} of 263.8 nm.

Preparation of praziquantel-loaded clay carrier. In order to determine the optimum MMT/PZQ ratio required to achieve maximum intercalation of drug into clay, four different 100-ml aqueous suspensions containing constant concentrations of clay powder were prepared and each of four different concentrations of praziquantel was added to each suspension at a constant temperature (60°C) and pH 4 under continuous stirring for 2 h to obtain four different formulations, F1 to F4, containing MMT/PZQ weight ratios of 1:1, 1:2, 1:3, and 1:4, respectively.

Characterization of the prepared praziquantel clay carrier. (i) Morphology and dimensions. The morphology and dimensions of the clay drug carrier were studied via transmission electron microscopy (TEM; JEM-1230; JEOL, Japan). The clay drug particles were dispersed in deionized water, and a drop of the liquid containing the dispersed nanoparticles was placed on the copper grid for TEM examination.

(ii) FTIR. The conjugation of praziquantel into clay was studied by recording Fourier transform infrared spectroscopy (FTIR) spectra (FT/IR-480) of clay, praziquantel, and clay-praziquantel hybrids (F1 to F4) at 4 cm^{-1} resolution.

(iii) EE. Each of the prepared MMT-PZQ mixtures was filtered, and the drug concentration in the filtrate was detected in triplicate using UV spectroscopy at a λ_{max} of 263.8 nm. The percentage of praziquantel entrapped in the MMT layers was determined using the equation entrapment efficiency (EE) = (amount of bound drug/total amount of drug) × 100.

***In vitro* release.** After 24 h of stirring of drug-clay mixtures as mentioned above, the praziquantel-loaded clay suspensions were freeze-dried using a Novalyphe-NL 500 (Savant Instruments Corp., USA) freeze-dryer to obtain dry powder. A weighed amount of each praziquantel-clay nanoparticle formulation (F1 to F4) equivalent to 20 mg praziquantel was secured in a non-rate-limiting cellulose acetate membrane bag and immersed in 750 ml of 0.1 N HCl at 37°C and 100 rpm using a USP dissolution tester, apparatus II. After specific intervals and up to 2 h, a 3-ml aliquot of samples was withdrawn and immediately replaced with the same amount of fresh medium. The praziquantel content in the aliquot was quantitatively analyzed by UV-visible (UV-vis) spectrophotometry at 263.8 nm. A commercially available praziquantel product was taken as the control. All the experiments were done in triplicate, and mean values were reported.

Biological assay. (i) Animals. Male Swiss albino mice obtained from the Schistosome Biological Supply Center (SBSC) of the Theodor Bilharz Research Institute (TBRI), Giza, Egypt, each weighing 18 ± 2 g, were used in this study. The approval of the TBRI ethics committee was received before the work was conducted. Animals were maintained on a standard commercial pellet diet and were kept under standard conditions at the SBSC animal unit. The animal experiments were conducted in accordance with the internationally valid animal ethics guidelines.

(ii) Animal groups for bioavailability study. For determining the bioavailability of the 1:1 clay-PZQ hybrid relative to a PZQ conventional product, four batches, each of 96 mice, were used. Two of the four batches were infected with 80 ± 10 *S. mansoni* cercariae/mouse using the body immersion technique (14) whereas the other two were kept uninfected. Both the uninfected and infected batches of mice were classified into groups depending on the form of PZQ given to assess the bioavailability of both the conventional PZQ and the clay-PZQ nanoformulation after their administration in a single oral dose of 500 mg/kg of body weight. Each of the four groups was further subdivided into 12 groups according to time of sacrifice, i.e., 2, 5, 15, 30, 60, 90, 120, 150, 180, 240, 360, and 480 min postdosing. After animal killing by decapitation, blood samples were collected and sera were separated by centrifugation at 1,850 × *g* for 10 min and stored at −70°C. For the PZQ concentration assay, 0.5 ml of sera was extracted with 3-ml aliquots of ethyl acetate and centrifuged at 1,850 × *g* for 15 min.

(iii) Estimation of the bioavailability of PZQ-MMT clay in sera. Estimation of PZQ in the different serum samples was done using high-performance liquid chromatography (HPLC; series 200 LC; PerkinElmer, USA). The column flow rate was adjusted to 2 ml/min, the mobile phase used was 37% acetonitrile-H_2O, and the detector wavelength was set at 210 nm. Two-milliliter aliquots of the extracts were evaporated to dryness at 25°C under a nitrogen stream, and the residue was then resuspended in 200 μl of acetonitrile and shaken on a vortex mixer for 1 min. Twenty microliters of sample was then injected into a Nova Pak C_{18}, 60-Å, 4-μm, 3.9- by 150-mm HPLC column (Waters Millipore Corp., USA) equipped with a programmable multiwavelength detector (series 200; PerkinElmer, USA). The calibration curve was linear between 0 and 6.4 μg/ml (correlation coefficient [r] = 0.9998). The coefficients of variation of the within- and interday reproducibility were 1 to 3% and 1 to 4%, respectively, depending on drug concentration.

(iv) Pharmacokinetic analysis. Pharm PCS software (version 4.2) was used for computing pharmacokinetic parameters based on the classic method of residuals and the least square technique for curve fitting (15). Coefficients and exponents of the fitted function were used to calculate the theoretical maximum concentration (C_{max}) and the time to maximum concentration (T_{max}) of PZQ. The corresponding elimination half-lives ($t_{1/2e}$) were calculated as ln 2/elimination rate constant (k_{el}). The area under the serum concentration-time curve (AUC_{0-8}) was calculated by applying the linear trapezoidal method.

***In vivo* efficacy study.** For the *in vivo* efficacy evaluation, 112 *S. mansoni*-infected mice (80 ± 10 cercariae/mouse) were divided into two groups of 56 mice each. Each group was further subdivided into seven subgroups, six of which were treated with either PZQ or clay-PZQ nanoformulation in doses of 31.25, 62.5, 125, 250, 500, and 1,000 mg/kg for five consecutive days starting from the 7th week after infection, while the seventh subgroup served as a control. The drug was dispersed in water

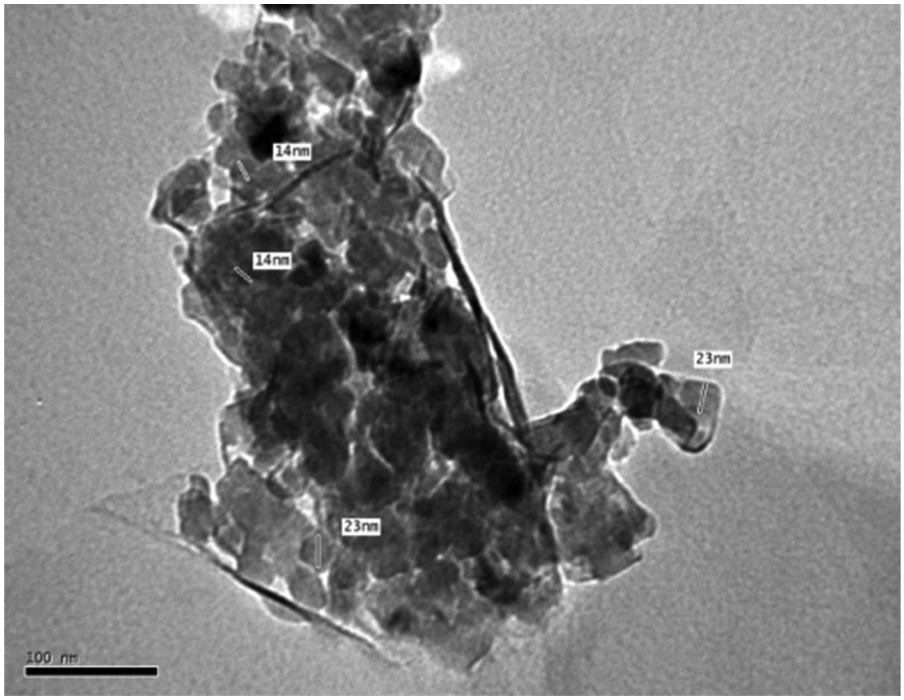

FIG 1 TEM image revealing the intercalation of PZQ into MMT.

with 2% Cremophor-EL (Sigma-Aldrich, St. Louis, MO, USA), a fresh batch of doses was prepared, and it was administered by oral gavage to each mouse according to each animal's body weight. Two weeks after the end of treatment (9 weeks postinfection), animals were sacrificed and perfused, and the worm burden was quantified (16) for estimation of percent worm reduction and assessment of PZQ 50% effective dose (ED_{50}) (17). After perfusion, a piece of liver and one of intestine were taken to count the number of eggs per gram of these tissues (18), while another piece of the small intestine was used to determine the percentage of the different egg developmental stages (19).

The percent reduction of worm burden in each treated group was calculated according to the equation % reduction = (no. of worms in control group − no. of worms in treated group)/(no. of worms in control group). ED_{50} (the effective dose of PZQ required to kill 50% of adult worms) values were calculated using Prism (GraphPad; version 3.03) computer software. Results were expressed as the mean ± standard error (SE). A two-tailed Student *t* test was used to detect the significance of differences between the means of different groups. Results were considered significant if the *P* value was <0.05.

RESULTS

Intercalation of PZQ in MMT nanocarrier. Intercalation of PZQ in MMT occurred rapidly due to ion-exchange reaction between the interlayer ions of the MMT and PZQ molecules. About 38% of PZQ was intercalated within 2 h of interaction time, and this percentage remained constant for 12 h; therefore, the intercalation time was set to 2 h in all preparations. The effect of pH on the intercalation of PZQ into the interlayer of MMT showed decreased intercalation of PZQ with a pH decrease below 3 due to largely uncharged PZQ species. pH 4 showed almost constant and stable intercalation of PZQ in MMT.

Characterization of the prepared praziquantel clay carrier. (i) Morphology and dimensions. The TEM image (Fig. 1) showed the MMT particles as sheets or wires (when the sheet is perpendicular to the grid) with the PZQ particles enclosed between the sheets.

(ii) FTIR. Fourier transform infrared spectroscopy (FTIR) spectra of MMT, PZQ, and PZQ-MMT clay hybrid are shown in Fig. 2. MMT shows the characteristic absorption bands at 3,400 cm^{-1} due to −OH stretching band for adsorbed water. The shoulders and broadness of the structural −OH band are mainly due to contributions of several structural −OH groups occurring in the MMT. The absorption peak (1,640 cm^{-1}) is attributed to −OH bending mode of adsorbed water. The characteristic peaks at 1,115 and 1,035 cm^{-1} are due to Si-O stretching vibrations out-of-plane and in-plane, respectively, for layered silicates. The peaks re-

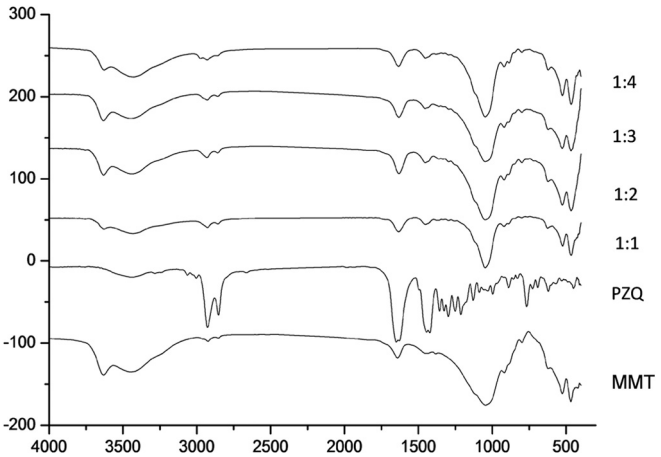

FIG 2 FTIR of MMT, PZQ, and PZQ-MMT clay hybrids in ratios of 1:1, 2:1, 3:1, and 4:1.

TABLE 1 Entrapment efficiency of MMT-PZQ hybrid

Formula	MMT/PZQ ratio	EE (%)
F1	1:1	75.90
F2	1:2	38.20
F3	1:3	32.67
F4	1:4	23.90

corded at 915, 875, and 836 cm^{-1} might be attributed to AlAlOH, AlFeOH, and AlMgOH bending vibrations, respectively (20).

For PZQ, the wide band in the region 3,600 to 3,400 cm^{-1} indicates a characteristic stretching of the O-H group which, in this case, can be attributed to the presence of water molecules. In the region 3,000 to 2,900 cm^{-1}, vibration absorption bands of C-H connections are seen, reflecting the symmetrical and asymmetric axial deformations of CH_2 and CH_3 groups. Stretching bands overlaid at 1,651 cm^{-1} represent two carbonyls (C = O) stretching absorption. At 1,437 cm^{-1}, CH_2 angular stretching symmetrical bands appear with a band overlap partially observed at 1,651 cm^{-1} for two connections stretching among carbons of the aromatic ring. Between 1,350 and 1,000 cm^{-1}, axial deformation occurs with band overlapping of C-N and C-H symmetrical angular stretching of CH_2.

In the IR spectra of PZQ-MMT clay hybrids, not only did the characteristic bands belonging to MMT and PZQ appear in the spectra but also several other bands appeared while others were deformed, indicating the strong interaction between PZQ and MMT layers.

Entrapment efficiency. The EEs of the MMT-PZQ hybrids of 1:1, 1:2, 1:3, and 1:4 are shown in Table 1. EE was within the range of 23.90 to 75.90% for different hybrid ratios. The intercalation of PZQ in MMT was found to be inversely affected by the initial drug concentration. As the initial drug concentration increased, the amount of intercalated drug decreased.

***In vitro* release.** The release test was carried out through suspending different MMT-PZQ hybrids together with the conventional PZQ product in phosphate-buffered saline (pH 1.2) under continuous stirring at 37°C for 3 h (Fig. 3). The total percent drug released 3 h after the start of the experiment was in the range of 33 to 56% for the MMT-PZQ hybrids versus 80.86% for the PZQ conventional product. All of the hybrids followed a zero-order release profile in the first 2 h of the release experiment as indicated by their R^2 values. The release of PZQ from MM-PZQ hybrid was generally found to be slow and persistent compared to the conventional product. Formula F1 (MMT-PZQ, 1:1) showed the highest percentage of drug release while F4 (MMT-PZQ, 1:4) showed the lowest percentage; these results conform well with the entrapment efficiency results where the release rate of the drug was merely dependent on the quantity of drug loaded onto the MMT layers. Formula F1 (MMT-PZQ, 1:1) was selected for the *in vivo* study.

Biological assay. (i) Bioavailability study. The current study of PZQ-MMT clay nanoparticle formulation bioavailability revealed higher PZQ concentrations in sera of both healthy and *S. mansoni*-infected mice than that recorded for the corresponding conventional PZQ. This was evidenced by increase of AUC_{0-8}, C_{max}, k_a, and $t_{1/2e}$ with a decrease in k_{el} versus the corresponding groups treated with the conventional PZQ. Uninfected and *S. mansoni*-infected mice treated with the PZQ-MMT clay nanoformulation showed increases in both AUC_{0-8} and C_{max} by 3.61- and 1.96-fold and 2.16- and 1.94-fold, respectively, with a decrease in k_{el} by 2.84- and 1.35-fold and increase in k_a and $t_{1/2e}$ by 2.11- and 1.51-fold and 2.86- and 1.34-fold, respectively, versus the corresponding groups treated with the conventional PZQ. Serum PZQ was still detectable at the later observation times in uninfected and *S. mansoni*-infected mice treated with the PZQ-MMT clay nanoformulation. Meanwhile, complete disappearance of PZQ was recorded in the sera of the uninfected and *S. mansoni*-infected animals treated with conventional PZQ at some of the observation periods examined (Table 2 and Fig. 4).

(ii) *In vivo* PZQ-MMT clay efficacy study. The percent worm reduction was significantly increased in *S. mansoni*-infected mice treated with the PZQ-MMT clay nanoformulation over that in mice treated with conventional PZQ. The calculated ED_{50} value after treatment of animals with total doses of 31.25, 62.5, 125, 250, 500, and 1,000 mg/kg was found to be 20.25 mg/kg in mice treated with PZQ-MMT clay nanoformulation compared to 74.07 mg/kg in mice treated with conventional PZQ (Fig. 5a and b). This enhanced efficacy was expressed also by the remarkable and significant reductions in total tissue egg load (hepatic and intestinal) with all administered doses compared to groups treated with conventional PZQ (Fig. 6). Moreover, there were significant decreases

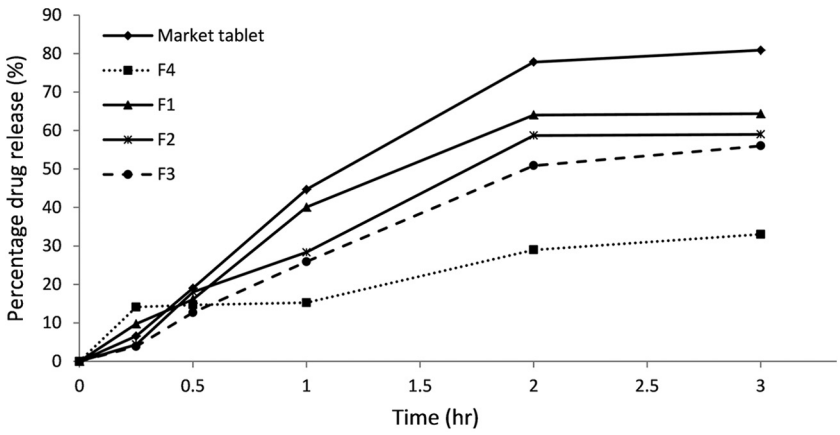

FIG 3 Release profile of PZQ from different MMT-PZQ formulations at pH 1.2.

TABLE 2 Pharmacokinetic parameters of PZQ-MMT clay nanoformulation versus conventional PZQ (500 mg/kg) in normal and *S. mansoni*-infected mice

Animal group	Treatment	Pharmacokinetic parameter (mean ± SEM)[a,b]					
		k_a (h^{-1})	k_{el} (h^{-1})	$t_{1/2e}$ (h^{-1})	AUC (μg · h/ml)	C_{max} (μg/ml)	T_{max} (h)
Normal	PZQ	6.44 ± 0.71	1.59 ± 0.07	0.44 ± 0.02	8.65 ± 0.88	14.34 ± 1.47	0.16 ± 0.03
	PZQ-MMT clay	13.59 ± 1.34***	0.56 ± 0.03***	1.26 ± 0.07***	31.19 ± 2.27***	30.93 ± 2.14***	0.12 ± 0.02
S. mansoni infected	PZQ	10.98 ± 1.35**	0.66 ± 0.05***	1.09 ± 0.08***	21.02 ± 1.91***	24.36 ± 2.12**	0.16 ± 0.02
	PZQ-MMT clay	16.62 ± 2.25 ‡	0.49 ± 0.04‡	1.46 ± 0.11‡	41.20 ± 3.94‡‡‡§	47.29 ± 2.44‡‡‡§§§	0.10 ± 0.02

[a] Abbreviations: k_{el}, elimination rate constant; $t_{1/2e}$, half-life time of elimination; AUC, area under concentration-time curve; C_{max}, *maximum concentration;* T_{max}, time to reach C_{max}.

[b] Symbols: ** and ***, significant differences versus PZQ-treated normal group at *P* values of <0.01 and <0.001, respectively; ‡ and ‡‡‡, significant differences versus PZQ-treated infected group at *P* values of <0.05 and <0.001, respectively; § and §§§, significant differences versus PZQ-MMT clay-treated normal group at *P* values of <0.05 and <0.001, respectively.

in total immature and mature eggs in mice treated with PZQ-MMT clay at doses 31.25, 125, and 250 mg/kg, respectively, and significant increase in dead eggs in mice treated at doses of 62.5, 125, and 250 mg/kg (Fig. 7).

DISCUSSION

Drugs for diseases of the poor are almost out of research focus due to the marginal or nearly nonexistent incentives. Consideration of existing compounds always simplifies and shortens the long and difficult process of discovering new drugs. PZQ is excellently endowed with antischistosomal activity. Enhancing PZQ bioavailability through its incorporation within a delivery system capable of controlling its delivery at a therapeutically optimal rate and dose may overcome some of its drawbacks and limitations. Nanosized novel drug delivery systems present a potential option to improve the performance of many existing drugs, an approach that may add to the significant potential cost savings, important in the context of drugs for these diseases (21).

In this work, higher efficacy was recorded in *S. mansoni*-infected mice treated with PZQ-MMT clay nanoformulation than in mice treated with conventional PZQ. This was shown by the increase in the percentage of worm reduction by 1- to 1.8-fold in infected mice treated with total doses of 31.25, 62.5, 125, 250, 500, and 1,000 mg/kg. Estimation of drug ED_{50} revealed less need for PZQ to achieve 50% killing of worms; the calculated ED_{50} for PZQ-MMT clay nanoformulation was reduced by more than 3-fold (20.25 mg/kg compared to 74.07 for conventional PZQ). This enhanced efficacy could be related to improved drug bioavailability overcoming some of its drawbacks, as PZQ is known to be rapidly and extensively absorbed after oral administration and is also rapidly eliminated (22). The extensive hepatic first-pass metabolism decreases tremendously its bioavailability.

Comparing the bioavailabilities of conventional PZQ between normal and *S. mansoni*-infected mice revealed increased drug bioavailability in *S. mansoni*-infected mice. These findings are in agreement with previous experiments (23, 24), and human studies (25–27) related such higher PZQ concentrations to the reduction of the concentration of cytochrome P450 (CYP450) and CYP450 reductase in mice and patients infected with *S. mansoni*. Inhibition of hepatic drug-metabolizing enzymes (CYP450 and cytochrome *b*5 [Cyt b_5]) activities in *S. mansoni*-infected mice was previously reported (24, 28–31).

Regarding the pharmacokinetic profile of PZQ in the clay nanoformulation, higher PZQ concentrations in sera of both normal and *S. mansoni*-infected mice were recorded with a significant increase in AUC_{0-8}, C_{max}, k_a, and $t_{1/2}$ and a decrease in k_{el}. Clays have been recently proposed as very useful materials for modulating drug delivery based on their unique layered structure, intercalation property, and high retention capacities as well as swelling and colloidal properties. Recently, new composite materials involving the interaction of drugs and inorganic clays have attracted considerable attention as sustained delivery carriers (12). Intercalation of organic molecules within the gallery of layered silicates

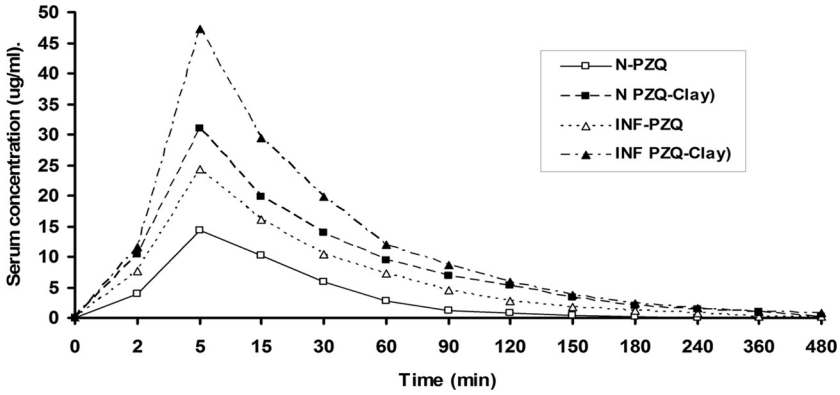

FIG 4 Serum concentration-time curves (micrograms per milliliter) of mice treated with a single oral dose (500 mg/kg) of PZQ and PZQ-MMT clay nanoformulation in normal (N) and *S. mansoni*-infected (INF) mice.

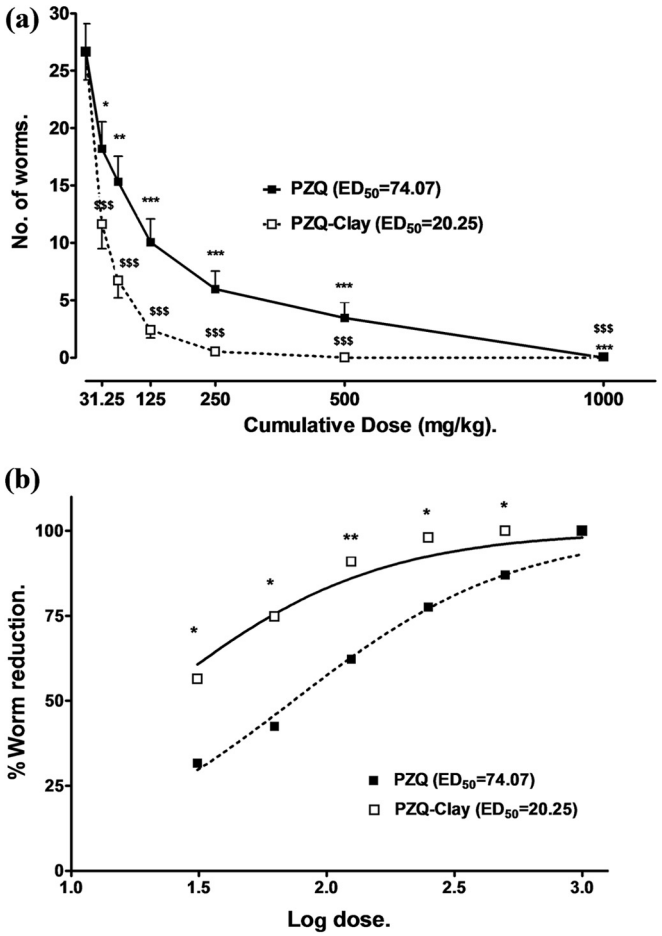

FIG 5 (a) Respective plots of the mean number of worms for conventional PZQ and PZQ-MMT clay in cumulative doses of 31.25, 62.5, 125, 250, 500, or 1,000 mg/kg compared to untreated control group (PZQ dose = 0). *, **, and ***, significant difference between PZQ-treated and untreated control group at *P* values of <0.05, <0.01, and <0.001, respectively. $$$, significant difference between PZQ-clay-treated and untreated control group at a *P* value of <0.001. (b) Computer-adjusted drug dose-response curves for conventional PZQ and PZQ-MMT clay. The curves were fitted to results calculated from panel a using Prism (GraphPad) software and were plotted assuming that they all had a minimum of 0% and a maximum of 100%. * and **, significant difference versus PZQ-treated group at *P* values of <0.05 and <0.01, respectively.

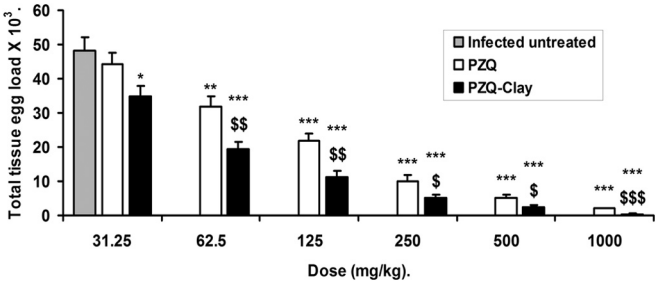

FIG 6 Total tissue egg load (hepatic and intestinal) in infected untreated mice and in mice treated with conventional PZQ and PZQ-MMT clay nanoformulation in doses of 31.25, 62.5, 125, 250, 500, and 1,000 mg/kg 9 weeks postinfection. *, **, and ***, significant versus infected untreated group at *P* values of <0.05, <0.01, and <0.001, respectively. $, $$, and $$$, significant versus PZQ-treated group at *P* values of <0.05, <0.01, and <0.001, respectively.

offers a novel route to prepare organic and inorganic hybrids that contain properties of both the inorganic host and the organic guest in a single material. MMT clay used in this work is a common ingredient both as an excipient and as an active substance in pharmaceutical products (12). It is a member of the smectite group, composed of silica tetrahedral sheets layered between alumina octahedral sheets. The imperfection of the crystal lattice and the isomorphous substitution inducing a net negative charge, leading to the adsorption of alkaline earth metal ions in the interlayer space, are responsible for the activity and exchange reactions with organic compounds. MMT also contains dangling hydroxyl end groups on the surfaces with a large specific surface area that helps to optimize adsorption ability and drug-carrying capability.

PZQ in clay nanoformulation used in this work possessed improved dissolution, solubility, and sustained release properties; the last may be related to the existence of electrostatic interactions between PZQ and the charges at the surface of MMT. The improved dissolution of PZQ is expected not only to enhance drug absorption but also to provide consistent absorption behavior and increase the period of residence of the drug in the systemic circulation and hence the time of exposure of the parasite to cysticidal doses of the drug. Improved dissolution of PZQ when administered in clay nanoformulation was demonstrated in this work, where PZQ was still detectable at later observation times in uninfected and *S. mansoni*-infected mice compared to complete disappearance of PZQ in sera of parallel groups of normal and infected mice treated with conventional PZQ. This improved property overcomes the shortcomings of PZQ, specifically the high hepatic extraction rate with first-pass effects and metabolization by cytochrome P450 (CYP 1A2, 2C19, and 3A4) (32) to the most abundant nonactive drug metabolite 4-hydroxycyclohexyl-carbonyl analogue. For PZQ, only the pharmacokinetic properties of the unchanged parent drug are the ones to be considered. Concerning conventional PZQ, immature (3- to 5-week-old) worms/younger forms are stated in references 8 and 17 to be less insulted by PZQ than adult worms as they are exposed to lower concentrations of unchanged PZQ in the systemic circulation than are more mature forms located in the liver. Moreover, high oral doses were stated by Becket et al. (33) to be a necessity to overcome the quick first-pass metabolism and thereby achieve sufficient drug concentrations at the larval tissue (7). The antischistosomal effect of PZQ is stated to relate not only to the absolute height of the maximal plasma concentration but also to the length of exposure to the drug (34).

Although it may be argued that the increased bioavailability of PZQ in the systemic circulation could be a result of portosystemic shunting, the conduct of this experiment early after infection makes this possibility almost nonexistent. To our knowledge, this is the first study regarding the pharmacokinetics of PZQ-MMT clay nanoformulation. Previous studies revealed higher drug efficacy when praziquantel was administered as a polyvinylpyrrolidone (PVP) solid dispersion (SD). This formulation of PZQ-PVP-SD when given orally to *S. mansoni*-infected mice in cumulative doses of 62.5, 125, 250, 500, and 1,000 mg/kg revealed increased percent worm reduction with all administered doses of 1- to 1.5-fold. PZQ-PVP-SD ED_{50} was recorded to be 40.92 mg/kg, versus 99.29 mg/kg for conventional PZQ. This was coupled with a significant reduction in total tissue eggs and a decrease in total immature and mature eggs with an increase in dead eggs

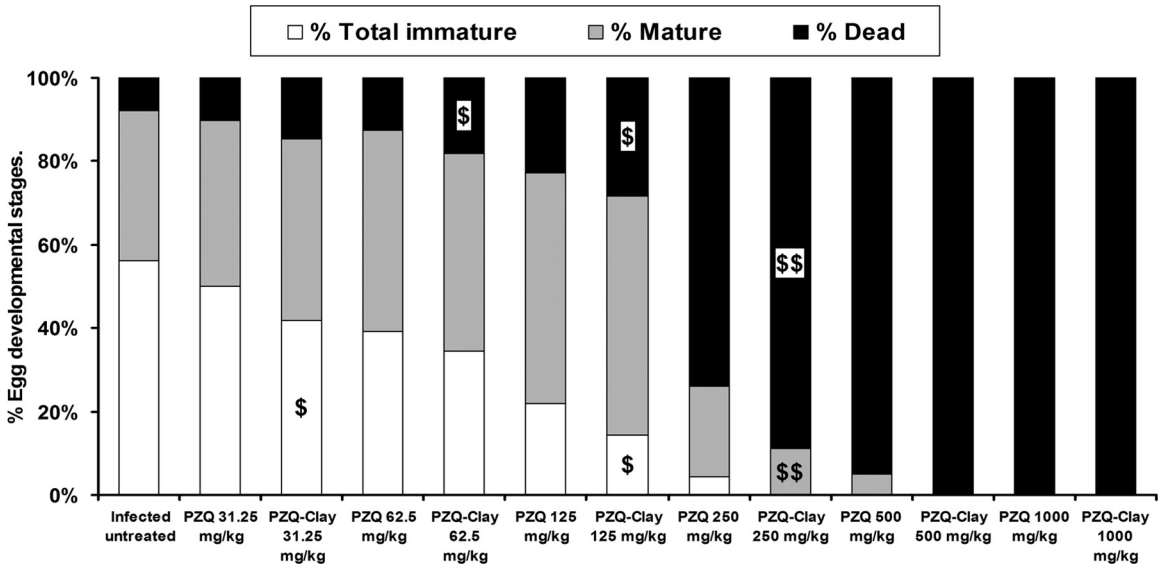

FIG 7 Percent egg developmental stages (oogram pattern) in infected untreated mice and in mice treated with conventional PZQ and PZQ-MMT clay nanoformulation in doses of 31.25, 62.5, 125, 250, 500, and 1,000 mg/kg 9 weeks postinfection. $ and $$, significant versus PZQ-treated group at P values of <0.05 and <0.01, respectively.

(35). Although polymer-based nanoparticles such as polylactide-coglycolide (PLGA) and polymeric micelles have been successfully utilized as drug carriers (36), the cost, physical instability, toxicity, and difficulties with large-scale production have precluded most from clinical applications. On the other hand, inorganic clay nanomaterials were found to possess the privilege of accommodating drugs between their layers, forming a variety of intercalated compounds. The intercalation of organic species (e.g., PZQ) into layered inorganic solids provides a convenient route to prepare organic-inorganic hybrids that contain properties of both the inorganic host and the organic guest in a single material: high specific surface area, adsorptive capacity, rheological properties, chemical inertness, and low or null toxicity (37) and power to effectively modulate and control drug release from drug-intercalated layered materials (21, 38).

In conclusion, PZQ-MMT clay nanoformulation provided a preparation with improved dissolution rate and thereby improved oral absorption and bioavailability. This improved bioavailability has been expressed in higher efficacy for the drug, where the dose necessary to kill 50% of the worms was reduced by >3-fold, with a longer period of drug residence in the systemic circulation, a property that may be of value in high-transmission areas where patients may be harboring immature parasites, the development of which into mature ones may favor the threat of resistant/tolerant parasites as a result of less exposure to the drug. This formulation overcomes several of the shortcomings of conventional PZQ. Moreover, MMT clay used in this work is a common ingredient both as an excipient and as an active substance in pharmaceutical products. Also, although conventional toxicity testing was not carried out in this work, animal mortalities were comparable between animals receiving conventional PZQ and PZQ-MMT clay, which may point to its safety.

REFERENCES

1. **World Health Organization.** 2013. Schistosomiasis. World Health Organization, Geneva, Switzerland.
2. **Meyer T, Sekljic H, Fuchs S, Bothe H, Schollmeyer D, Miculka C.** 2009. Taste, a new incentive to switch to (R)-praziquantel in schistosomiasis treatment. PLoS Negl Trop Dis **3:**e357. http://dx.doi.org/10.1371/journal.pntd.0000357.
3. **Carabin H, Guyatt H, Engels D.** 2000. A comparative analysis of the cost-effectiveness of treatment based on parasitological and symptomatic screening for Schistosoma mansoni in Burundi. Trop Med Int Health **5:**192–202. http://dx.doi.org/10.1046/j.1365-3156.2000.00530.x.
4. **Akbarieh M, Besner JG, Galal A, Tawashi R.** 1992. Liposomal system for the targeting and controlled release of praziquantel. Drug Dev Ind Pharm **18:**303–317. http://dx.doi.org/10.3109/03639049209043701.
5. **El-Arini SK, Leuenberger H.** 1998. Dissolution properties of praziquantel-PVP systems. Pharm Acta Helv **73:**89–94. http://dx.doi.org/10.1016/S0031-6865(97)00051-4.
6. **Lindenberg M, Kopp S, Dressman JB.** 2004. Classification of orally administered drugs on the World Health Organization model list of essential medicines according to the biopharmaceutics classification system. Eur J Pharm Biopharm **58:**265–278. http://dx.doi.org/10.1016/j.ejpb.2004.03.001.
7. **Mourão SC, Costa PI, Salgado HRN, Gremião MPD.** 2005. Improvement of antischistosomal activity of praziquantel by incorporation into phosphatidylcholine-containing liposomes. Int J Pharm **295:**157–162. http://dx.doi.org/10.1016/j.ijpharm.2005.02.009.
8. **Xiao SH, Catto BA, Webster LT.** 1985. Effects of praziquantel on different developmental stages of Schistosoma mansoni in vitro and in vivo. J Infect Dis **151:**1130–1137. http://dx.doi.org/10.1093/infdis/151.6.1130.
9. **Chai JY.** 2013. Praziquantel treatment in trematode and cestode infections: an update. Infect Chemother **45:**32–43. http://dx.doi.org/10.3947/ic.2013.45.1.32.
10. **Greenberg RM.** 2013. New approaches for understanding mechanisms of drug resistance in schistosomes. Parasitology **140:**1534–1546. http://dx.doi.org/10.1017/S0031182013000231.
11. **Ridley RG.** 2003. Product R&D for neglected diseases. Twenty-seven years of WHO/TDR experiences with public-private partnerships. EMBO Rep **4**(Suppl 1)**:**S43–S46. http://dx.doi.org/10.1038/sj.embor.embor858.
12. **Wang X, Du Y, Luo J.** 2008. Biopolymer/montmorillonite nanocomposite: preparation, drug-controlled release property and cytotoxicity. Nanotechnology **19:**065707. http://dx.doi.org/10.1088/0957-4484/19/6/065707.
13. **Bergaya F, Theng BKG, Lagaly G.** 2006. Handbook of clay science, 1st ed. Elsevier Publications, Amsterdam, The Netherlands.
14. **Liang YS, John BI, Boyd DA.** 1987. Laboratory cultivation of schistosome vector snails and maintenance of schistosome life cycles. Proc 1st Sino-Am Symp **1:**34–48.

15. **Gibaldi M, Perrier D.** 1982. Pharmacokinetics. 2nd ed. Marcel Dekker Inc, New York, NY.
16. **Duvall RH, De Witt WB.** 1967. Technique for recovering adult schistosomes from laboratory animals. Am J Trop Med Hyg **16:**438–486.
17. **Cioli D, Botros S, Wheatcroft-Francklow K, Mbaye A, Southgate V, Tchuente LA, Pica-Mattoccia L, Troiani AR, el-Din SH, Sabra A, Albin J, Engels D, Doenhoff M.** 2004. Determination of ED50 values for praziquantel in praziquantel-resistant and susceptible Schistosoma mansoni isolates. Int J Parasitol **34:**979–987. http://dx.doi.org/10.1016/j.ijpara.2004.05.001.
18. **Cheever AW.** 1968. Conditions affecting the accuracy of potassium hydroxide digestion techniques for counting Schistosoma mansoni eggs in tissues. Bull World Health Organ **39:**328–331.
19. **Pellegrino J, Oliveira CA, Faria J, Cunha AS.** 1962. New approach to the screening of drugs in experimental schistosomiasis mansoni in mice. Am J Trop Med Hyg **11:**201–215.
20. **Patel HA, Somani RS, Bajaj HC, Jasra RV.** 2007. Preparation and characterization of phosphonium montmorillonite with enhanced thermal stability. Appl Clay Sci **35:**194. http://dx.doi.org/10.1016/j.clay.2006.09.012.
21. **Zheng JP, Luan L, Wang HY, Xi LF, Yao KD.** 2007. Study on ibuprofen/montmorillonite intercalation composites as drug release system. Appl Clay Sci **36:**297. http://dx.doi.org/10.1016/j.clay.2007.01.012.
22. **Hong ST, Lee SH, Lee SJ, Kho WG, Lee M, Li S, Chung BS, Seo M, Choi MH.** 2003. Sustained-release praziquantel tablet: pharmacokinetics and the treatment of clonorchiasis in beagle dogs. Parasitol Res **91:**316–320. http://dx.doi.org/10.1007/s00436-003-0958-7.
23. **Andrews P, Dycka J, Frank G.** 1980. Effect of praziquantel on clinical chemical parameters in healthy and schistosome-infected mice. Ann Trop Med Parasitol **74:**167–177.
24. **Botros SS, Seif el-Din SH, El-Lakkany NM, Sabra AA, Ebeid FA.** 2006. Drug metabolizing enzymes and praziquantel bioavailability in mice harboring Schistosoma mansoni isolates of different drug susceptibilities. J Parasitol **92:**1344–1349. http://dx.doi.org/10.1645/GE-865R.1.
25. **El-Guiniady MA, El-Touny MA, Abdel-Bary MA, Abdel-Fatah SA, Metwally AA.** 1994. Clinical and pharmacokinetic study of praziquantel in Egyptian schistosomiasis patients with and without liver cell failure. Am J Trop Med Hyg **51:**809–818.
26. **Brant PC, Prata A.** 1979. Altered drug metabolism in hepatosplenic schistosomiasis. Rev Inst Med Trop Sao Paulo **21:**254–259.
27. **Tekwanl BL, Shukla OP, Ghatak S.** 1988. Altered drug metabolism in parasitic diseases. Parasitol Today **4:**4–10. http://dx.doi.org/10.1016/0169-4758(88)90047-6.
28. **Sheweita SA, Mangoura SA, El-Shemi AG.** 1998. Different levels of Schistosoma mansoni infection induced changes in drug-metabolizing enzymes. J Helminthol **72:**71–77. http://dx.doi.org/10.1017/S0022149X00001012.
29. **Ebeid FA, Seif el-Din SH, Ezzat AR.** 2000. Effect of Schistosoma mansoni infection and treatment on drug-metabolizing enzymes. Arzneimittelforschung **50:**867–874.
30. **El-Lakkany NM, Seif el-Din SH, Badawy AA, Ebeid FA.** 2004. Effect of artemether alone and in combination with grapefruit juice on hepatic drug-metabolizing enzymes and biochemical aspects in experimental Schistosoma mansoni. Int J Parasitol **34:**1405–1412. http://dx.doi.org/10.1016/j.ijpara.2004.08.012.
31. **Botros S, El-Lakkany N, Seif el-Din SH, Sabra A, Ibrahim M.** 2011. Comparative efficacy and bioavailability of different praziquantel brands. Exp Parasitol **127:**515–521. http://dx.doi.org/10.1016/j.exppara.2010.10.019.
32. **Li X-Q, Bjorkman A, Andersson TB, Gustafsson LL, Masimirembwa CM.** 2003. Identification of human cytochrome P450s that metabolise anti-parasitic drugs and predictions of in vivo drug hepatic clearance from in vitro data. Eur J Clin Pharmacol **59:**429–442. http://dx.doi.org/10.1007/s00228-003-0636-9.
33. **Becket G, Schep LJ, Tan MY.** 1999. Improvement of the *in vitro* dissolution of praziquantel by complexation with α, β and γ cyclodextrins. Int J Pharm **179:**65–71. http://dx.doi.org/10.1016/S0378-5173(98)00382-2.
34. **Gonnert R, Andrews P.** 1977. Praziquantel, a new broad-spectrum antischistosomal agent. Z Parasitenkd **52:**129–150. http://dx.doi.org/10.1007/BF00389899.
35. **El-Lakkany N, Seif El-Din SH, Heikal L.** 2012. Bioavailability and in vivo efficacy of a praziquantel-polyvinylpyrrolidone solid dispersion in Schistosoma mansoni-infected mice. Eur J Drug Metab Pharmacokinet **37:**289–299. http://dx.doi.org/10.1007/s13318-012-0089-6.
36. **Cohen-Sela E, Dangoor D, Epstein H, Gati I, Danenberg HD, Golomb G, Gao J.** 2006. Nanospheres of a bisphosphonate attenuate intimal hyperplasia. J Nanosci Nanotechnol **6:**3226–3234. http://dx.doi.org/10.1166/jnn.2006.428.
37. **Mohanambe L, Vasudevan S.** 2005. Anionic clays containing anti-inflammatory drug molecules: comparison of molecular dynamics simulation and measurements. J Phys Chem B **109:**15651–15658. http://dx.doi.org/10.1021/jp050480m.
38. **Lin FH, Lee YH, Jian CH, Wong JM, Shieh MJ, Wang CY.** 2002. A study of purified montmorillonite intercalated with 5-fluorouracil as drug carrier. Biomaterials **23:**1981. http://dx.doi.org/10.1016/S0142-9612(01)00325-8.